J. Fluid Mech. (1981), *vol.* 105, *part* 9, *pp.* 469–486
Printed in Great Britain

A delay-diffusion description for contaminant dispersion

By RONALD SMITH

Department of Applied Mathematics and Theoretical Physics,
University of Cambridge, Silver Street, Cambridge CB3 9EW

(Received 22 November 1979 and in revised form 11 August 1980)

The rate of longitudinal dispersion of a contaminant in a current depends upon concentration variations across the flow. These variations are generated by the combination of a longitudinal concentration gradient and a cross-stream velocity shear. However, the response is not instantaneous and so not only is the dispersion coefficient $D(\tau)$ time-dependent, but also there is a memory of the concentration distribution at earlier times. In this paper it is shown that these features are accurately reproduced by the delay-diffusion equation

$$\partial_t \bar{c} + \bar{u}\,\partial_x \bar{c} - \bar{\kappa}\,\partial_x^2 \bar{c} - \int_0^\infty \partial_\tau D\,\partial_x^2 \bar{c}\left(x - \int_0^\tau \tilde{u}(\tau')\,d\tau', t-\tau\right) d\tau = \bar{q}(x,t),$$

where $\bar{q}$ is the source strength, $\bar{u}$ the bulk velocity and $\tilde{u}$ a transport velocity for the free decay of cross-stream concentration variations.

1. Introduction

Taylor (1953, 1954) showed that after a sufficient length of time has elapsed, the longitudinal dispersion of a contaminant in a laterally confined flow is governed by a constant-coefficient diffusion equation. Unfortunately, in many applications there is insufficient time available for this asymptotic state to be reached. Indeed, some of Taylor's own experiments are not consistent with his theory (Chatwin 1971).

To remedy this shortcoming Gill & Sankarasubramanian (1970) have advocated that a variable coefficient diffusion equation

$$\partial_t \bar{c} + \hat{u}(t)\,\partial_x \bar{c} - [\kappa + D(t)]\,\partial_x^2 \bar{c} = 0, \tag{1.1}$$

be used to model all stages of the dispersion process. Relying upon this hypothesis they have calculated the necessary time dependence of the transport velocity $\hat{u}(t)$ and of the shear dispersion coefficient $D(t)$. Equation (1.1) has the remarkable properties that the area, centroid and variance of the bulk concentration distribution $\bar{c}(x,t)$ are all exact. Moreover, the inclusion of systematic correction terms

$$-\sum_{i=3}^{\infty} K_i(t)\,\partial_x^i \bar{c} \tag{1.2}$$

(Gill & Sankarasubramanian 1970) leads to exact results for the higher-order moments also (De Gance & Johns 1978).

In a severe criticism of variable diffusivity equations, Taylor (1959) pointed out that when there are discharges at several times the dispersion coefficient must simultaneously have several different values. Gill & Sankarasubramanian (1972) show how

this mathematical complication can be dealt with. However, it is difficult to reconcile the equations with the underlying physical processes. Taylor (1959) concluded 'It seems therefore that no physical meaning can be attached to the use of equations in which the coefficient of diffusion varies with the time of diffusion, even though the formulae produced by their use do represent adequately the concentrations in particular cases'.

The longitudinal dispersion equation has its origins in the cross-sectionally averaged advection–diffusion equation

$$\partial_t \bar{c} + \bar{u}\,\partial_x \bar{c} + \partial_x[\overline{(u-\bar{u})(c-\bar{c})}] - \kappa\,\partial_x^2 \bar{c} = \bar{q}. \tag{1.3}$$

Here c is the concentration, u the longitudinal velocity, κ the molecular diffusivity, $\bar{q}$ the source strength, and over-bars denote cross-sectional average values. Thus, as was first recognized by Taylor (1953), the essential ingredient for a bulk model is an expression for the cross-sectional variations of concentration $c-\bar{c}$ in terms of $\bar{c}$.

Shear distortion can be thought of as twisting longitudinal gradients over into lateral gradients. At large times after contaminant release this leads to $c-\bar{c}$ being proportional to $\partial_x \bar{c}$ (Taylor 1953). Guided by this asymptotic result Gill & Sankarasubramanian (1970) proposed the representation

$$c-\bar{c} = \sum_{j=1}^{\infty} f_j(y,z,t)\,\partial_x^j \bar{c}(x,t). \tag{1.4}$$

Thus, the concentration variations across the flow are related to the gradient of the instantaneous local bulk concentration. Substitution of this representation into equation (1.3) yields the composite equation (1.1), (1.2).

The basis of the present work is the recognition that at small times after contaminant release, equation (1.4) is not an efficient representation of the cross-stream dispersion. There is only a gradual response to the continuing generation of lateral concentration gradients via the velocity shear. Moreover, the transport velocity for the free decay of lateral concentration gradients is different from the bulk velocity (i.e. an average of the velocity profile weighted towards regions of higher concentration gradient). This leads us to pose the new ansatz

$$c-\bar{c} = \sum_{j=1}^{\infty} \int_0^{\infty} l_j(y,z,\tau)\,\partial_x^j \bar{c}\left(x - \int_0^{\tau} \tilde{u}(\tau')\,d\tau', t-\tau\right) d\tau. \tag{1.5}$$

Thus, there is a fading advected memory of the concentration gradient at earlier times.

At the lowest-order truncation ($j=1$) substitution of the representation (1.5) into equation (1.3) leads to the delay-diffusion equation

$$\partial_t \bar{c} + \bar{u}\,\partial_x \bar{c} - \kappa\,\partial_x^2 \bar{c} - \int_0^{\infty} \partial_\tau D\,\partial_x^2 \bar{c}\left(x - \int_0^{\tau} \tilde{u}(\tau')\,d\tau', t-\tau\right) d\tau = \bar{q}(x,t). \tag{1.6}$$

Consistency between the alternative representations (1.4), (1.5) requires that

$$l_1 = \partial_\tau f_1. \tag{1.7}$$

This is why the delay-dispersion function $\partial_\tau D$ in equation (1.6) is the time derivative of the shear-dispersion coefficient $D(\tau)$. This close connexion with equation (1.1) also leads to the area, centroid and variance for $\bar{c}(x,t)$ being exact. Indeed, with the optimal choice for $\tilde{u}(\tau')$ the skewness is also exact.

The crucial new feature of equation (1.6) is that there is no restriction to sudden discharges at a single point in time. The rate of dispersion associated with earlier discharges is relatively large because the memory term extends further back in time. Equivalently, the concentration variations across the flow have had more time to approach equilibrium with the generation mechanism.

2. Longitudinal and transverse dispersion equations

As the starting point for our mathematical analysis we take the full equations to have the form

$$\left.\begin{aligned} &\partial_t c + u(y,z)\,\partial_x c - \kappa\,\partial_x^2 c - \nabla.(\kappa\nabla c) = \bar{q}(x,t) \\ &\text{with} \\ &\kappa\mathbf{n}.\nabla c = 0 \quad \text{on} \quad \partial A. \end{aligned}\right\} \tag{2.1}$$

Here $\kappa(y,z)$ is the diffusivity, ∇ the two-dimensional gradient operator (∂_y, ∂_z), $\mathbf{n}$ the outward normal, ∂A the impermeable boundary, and $\bar{q}$ the uniform discharge rate. For simplicity the analysis of non-uniform discharges is deferred to a later paper.

If the ansatz (1.5) is substituted into the cross-sectionally averaged form of the dispersion equation (2.1), then we arrive at the integro-differential equation

$$\partial_t \bar{c} + \bar{u}\,\partial_x \bar{c} - \bar{\kappa}\,\partial_x^2 \bar{c} + \sum_{j=1}^{\infty} \int_0^{\infty} \overline{l_j(u-\bar{u})}\,\partial_x^{j+1}\bar{c}\left(x - \int_0^{\tau} \tilde{u}, t-\tau\right) d\tau - \sum_{j=1}^{\infty} \int_0^{\infty} \overline{(\kappa-\bar{\kappa})\,l_j}\,\partial_x^{j+2}\bar{c}\left(x - \int_0^{\tau} \tilde{u}, t-\tau\right) d\tau = \bar{q}. \tag{2.2}$$

Here, by comparison with equation (1.3), we have included extra terms which arise when the diffusivity κ is non-constant. We note that the higher-order terms in equation (2.2) depend only upon the concentration profile at previous times. Thus, the essential mathematical character is determined by the $(\partial_t + \bar{u}\,\partial_x - \kappa\,\partial_x^2)$ terms, and it is acceptable to truncate the l_j series at any level. Of course, our analysis is directed towards making a truncation quantitatively as well as qualitatively acceptable.

By design, the structure of the series (1.5) is preserved under differentiation. In particular, using integration by parts with respect to τ, we can derive the expression

$$\partial_t c = \partial_t \bar{c} + \sum_{j=1}^{\infty} l_j(y,z,0)\,\partial_x^j \bar{c} + \sum_{j=1}^{\infty} \int_0^{\infty} (\partial_\tau l_j - \tilde{u}(\tau)\,l_{j-1})\,\partial_x^j \bar{c}\left(x - \int_0^{\tau} \tilde{u}(\tau')\,d\tau', t-\tau\right) d\tau, \tag{2.3}$$

where the series expansion for $\partial_t \bar{c}$ is given by equation (2.2) above. Thus, written in full, the field equations and boundary conditions (2.1) for the contaminant dispersion become

$$\left.\begin{aligned} &[l_1(y,z,0) + u - \bar{u}]\,\partial_x \bar{c} + [l_2(y,z,0) + \bar{\kappa} - \kappa]\,\partial_x^2 \bar{c} + \sum_{j=3}^{\infty} l_j(y,z,0)\,\partial_x^j \bar{c} \\ &+ \sum_{j=1}^{\infty} \int_0^{\infty} [\partial_\tau l_j - \tilde{u}(\tau)\,l_{j-1} + u l_{j-1} - \overline{u l}_{j-1} - \kappa l_{j-2} \\ &+ \overline{\kappa l}_{j-2} - \nabla.(\kappa\nabla l_j)]\,\partial_x^j \bar{c}\left(x - \int_0^{\tau} \tilde{u}(\tau')\,d\tau', t-\tau\right) d\tau = 0 \\ &\text{with} \\ &\sum_{j=1}^{\infty} \int_0^{\infty} \kappa\mathbf{n}.\nabla l_j\,\partial_x^j \bar{c}\left(x - \int_0^{\tau} \tilde{u}(\tau')\,d\tau', t-\tau\right) d\tau = 0 \quad \text{on} \quad \partial A. \end{aligned}\right\} \tag{2.4}$$

Since the solution procedure must be valid for any $\bar{c}$ profile, it is natural to require that the individual equations corresponding to each $\partial_x^j \bar{c}$ coefficient and integrand be satisfied separately. This prescription leads to the sequence of initial-boundary-value problems

$$\left.\begin{aligned} &\partial_\tau l_1 - \nabla.(\kappa \nabla l_1) = 0, \\ \text{with}\quad &\kappa \mathbf{n}.\nabla l_1 = 0 \quad \text{on} \quad \partial A, \quad \text{and} \quad l_1 = \bar{u} - u \quad \text{at} \quad \tau = 0, \end{aligned}\right\} \tag{2.5}$$

$$\left.\begin{aligned} &\partial_\tau l_2 - \nabla.(\kappa \nabla l_2) = \tilde{u}(\tau) l_1 + (\overline{u l_1} - u l_1), \\ \text{with}\quad &\kappa \mathbf{n}.\nabla l_2 = 0 \quad \text{on} \quad \partial A, \quad \text{and} \quad l_2 = \kappa - \bar{\kappa} \quad \text{at} \quad \tau = 0, \end{aligned}\right\} \tag{2.6}$$

$$\left.\begin{aligned} &\partial_\tau l_j - \nabla.(\kappa \nabla l_j) = \tilde{u}(\tau) l_{j-1} + (\overline{u l_{j-1}} - u l_{j-1}) + (\kappa l_{j-2} - \overline{\kappa l_{j-2}}), \\ \text{with}\quad &\kappa \mathbf{n}.\nabla l_j = 0 \quad \text{on} \quad \partial A, \quad \text{and} \quad l_j = 0 \quad \text{at} \quad \tau = 0. \end{aligned}\right\} \tag{2.7}$$

The physical interpretation of these equations is as a description of longitudinally uniform cross-sectional contaminant variations. The initial values and the forcing terms are analogues of the generation mechanism of non-uniform advection.

By induction we can infer that the initial growth rates of the weight functions are

$$\left.\begin{aligned} l_{2j} &= O(\tau^j), \quad l_{2j+1} = O(\tau^j) \quad \text{when} \quad \kappa = \bar{\kappa}, \\ l_{2j} &= O(\tau^{j-1}), l_{2j+1} = O(\tau^j) \quad \text{when} \quad \kappa \neq \bar{\kappa}. \end{aligned}\right\} \tag{2.8}$$

Thus, as is also the case with Gill and Sankarasubramanian's method, for small times it is the low derivative terms in the bulk equation (2.2) which gives the largest contribution to the shear dispersion. Conversely, at large times we can expect that the ever-increasing length scale of the contaminant distribution $\bar{c}(x, t)$ ensures that the higher derivatives are small, and again the low-derivative terms are dominant.

3. Delay-dispersion function

The eigenfunctions ψ_m for the decay of lateral concentration variations provide a convenient means of solving equation (2.5). These functions satisfy the eigenvalue problem

$$\left.\begin{aligned} &\nabla.(\kappa \nabla \psi_m) + \lambda_m \psi_m = 0, \\ \text{with}\quad &\kappa \mathbf{n}.\nabla \psi_m = 0 \quad \text{on} \quad \partial A. \end{aligned}\right\} \tag{3.1}$$

The lowest mode $\psi_0 = 1$ has $\lambda_0 = 0$ and corresponds to the steady state of a cross-sectionally uniform concentration distribution. To represent the velocity profile $u(y, z)$ we introduce the coefficients

$$u_m = \overline{u\psi_m}/(\overline{\psi_m^2})^{\frac{1}{2}}. \tag{3.2}$$

From the eigenfunction representation of the initial conditions, it is clear that the solution $l_1(y, z, \tau)$ of the homogeneous equation (2.5) can be written

$$l_1 = -\sum_{m=1}^{\infty} u_m \exp(-\lambda_m \tau)\{\psi_m(y, z)/(\overline{\psi_m^2})^{\frac{1}{2}}\}. \tag{3.3}$$

Also, in terms of u_m the delay-dispersion function in the lowest-order truncation of the bulk equation (2.2) is given by

$$\partial_\tau D = \overline{l_1(\bar{u}-u)} = \sum_{m=1}^{\infty} u_m^2 \exp(-\lambda_m \tau). \tag{3.4}$$

If Reynolds' analogy is applicable, and there is a constant ratio between the diffusivity κ and the viscosity ν, then we can derive a general expression for u_m. Our starting point is the longitudinal momentum equation

$$\left.\begin{aligned} \nabla.(\nu\nabla u) &= -G, \\ u &= 0 \quad \text{on} \quad \partial A, \end{aligned}\right\} \tag{3.5}$$

with

where $-G$ is the longitudinal pressure gradient. Multiplying the field equation by ψ_m, and repeatedly applying the divergence theorem we finally arrive at the result

$$u_m = -\frac{G(\kappa/\nu)}{\lambda_m} \int_{\partial A} \psi_m (\nu \nabla u.\mathbf{n})\, ds / (\overline{\psi_m^2})^{\frac{1}{2}} \int_{\partial A} (\nu \nabla u.\mathbf{n})\, ds. \tag{3.6}$$

Thus, to calculate u_m it suffices that we know the distribution of the drag forces $\nu\nabla u.\mathbf{n}$ around the boundary.

4. Selection of the velocity shift

Proceeding to the non-homogeneous problem (2.6) for $l_2(y,z,\tau)$ we introduce further coefficients

$$u_{mn} = \overline{u\psi_m\psi_n}/(\overline{\psi_m^2})^{\frac{1}{2}}(\overline{\psi_n^2})^{\frac{1}{2}}, \quad k_m = \overline{\kappa\psi_m}/(\overline{\psi_m^2})^{\frac{1}{2}}. \tag{4.1}$$

Thus, if we represent $l_2(y,z,\tau)$ by the eigenfunction expansion

$$l_2(y,z,\tau) = \sum_{m=1}^{\infty} a_m(\tau) \exp(-\lambda_m \tau) \{\psi_m(y,z)/(\overline{\psi_m^2})^{\frac{1}{2}}\}, \tag{4.2}$$

then the amplitude factors $a_m(\tau)$ satisfy the ordinary differential equations

$$\left.\begin{aligned} \partial_\tau a_m &= \sum_{n=1}^{\infty} u_{mn} u_n \exp((\lambda_m - \lambda_n)\tau) - \tilde{u}(\tau) u_m, \\ a_m &= k_m \quad \text{at} \quad \tau = 0. \end{aligned}\right\} \tag{4.3}$$

with

The solution can be written

$$a_m = k_m + u_m \left(u_{mm}\tau - \int_0^\tau \tilde{u}(\tau')\, d\tau'\right) + \sum_{n \neq m} u_{mn} u_n \left\{\frac{\exp((\lambda_m - \lambda_n)\tau) - 1}{\lambda_m - \lambda_n}\right\}, \tag{4.4}$$

and is explicitly dependent upon the chosen value of the velocity shift $\tilde{u}(\tau')$.

What we ideally would wish to achieve with our choice for $\tilde{u}(\tau')$ is that the solutions of the approximate equation (1.6) should be as close as possible to the solutions of the exact equation (2.1). Unfortunately, it is only in exceptional cases that the exact solution is available. Instead, we shall pursue the approximate analysis to one further level and use this higher-order equation as the basis for selecting $\tilde{u}(\tau')$.

Substituting the eigenfunction representation for l_1, l_2 and κ_1 into the bulk equation (2.2) we find that the integrand for the $\partial_x^3 \bar{c}$ contribution to the dispersion is given by

$$\overline{l_1(\overline{\kappa}-\kappa)} + \overline{l_2(u-\overline{u})}$$

$$= \sum_{m=1}^{\infty} k_m u_m \exp(-\lambda_m \tau) + \sum_{m=1}^{\infty} \left(u_{mm}\tau - \int_0^{\tau} \tilde{u}(\tau')\, d\tau' \right) u_m^2 \exp(-\lambda_m \tau)$$

$$+ \sum_{m=1}^{\infty} \sum_{n \neq m} u_n u_m u_{mn} \left\{ \frac{\exp(-\lambda_n \tau) - \exp(-\lambda_m \tau)}{\lambda_m - \lambda_n} \right\}. \tag{4.5}$$

The first term on the right-hand side shows the effect of lateral variations in the diffusivity, and the next two terms represent a higher-approximation to the shear effects than is given by the delay-dispersion function (3.4). Clearly, the optimal choice for $\tilde{u}$ is to make the correction for shear effects be identically zero

$$\partial_\tau D \int_0^{\tau} [\tilde{u}(\tau') - \overline{u}]\, d\tau' = \tau \sum_{m=1}^{\infty} [u_{mm} - \overline{u}] u_m^2 \exp(-\lambda_m \tau)$$

$$+ \sum_{m=1}^{\infty} \sum_{n \neq m} u_n u_m u_{mn} \left\{ \frac{\exp(-\lambda_n \tau) - \exp(-\lambda_m \tau)}{\lambda_m - \lambda_n} \right\}. \tag{4.6}$$

In particular, in the limits of small and of large times we have

$$\tilde{u}(0) = \overline{u} + \overline{(u-\overline{u})^3} / \overline{(u-\overline{u})^2}, \quad \tilde{u}(\infty) = u_{11}. \tag{4.7}$$

It can readily be inferred that when $\tilde{u}(\tau')$ is less than $\overline{u}$ the solutions of the new model equation (1.6) tend to become skewed toward the point of release. At the front the shear term 'remembers' the much weaker gradients far forward of the centroid and the contaminant flux is correspondingly reduced. Conversely, far to the rear the shear term 'remembers' the higher gradients close to the centroid and the contaminant flux is increased. Hence, the front remains relatively steep while the rear of the contaminant distribution is drawn out.

The extent of the skewness depends upon the difference between $\tilde{u}$ and $\overline{u}$. Thus, the accuracy of equation (1.6) hinges upon the selection of $\tilde{u}(\tau')$. When $\kappa = \overline{\kappa}$ the choice (4.6) for $\tilde{u}(\tau')$ ensures that the skewness is exact. To show this, we note that if we multiply the bulk equation (2.2) by x^n and repeatedly integrate by parts, then only the terms up to $\partial_x^n \bar{c}$ contribute to the nth moment $\bar{c}^{(n)}$. When $\kappa = \overline{\kappa}$ the optimal choice (4.6) eliminates the $\partial_x^3 \bar{c}$ term and so the one-term truncation (1.6) encompasses the next approximation also. Hence the area, centroid, variance and skewness are all exact. For later reference we record that in axes moving with the bulk velocity $\overline{u}$ the equations for the second and third moments $\bar{c}^{(2)}, \bar{c}^{(3)}$ take the form

$$\partial_t \bar{c}^{(2)} = 2\{\overline{\kappa} + D(t)\} \bar{c}^{(0)}, \tag{4.8}$$

$$\partial_t \bar{c}^{(3)} = 6\bar{c}^{(0)} \int_0^t \partial_\tau D \int_0^{\tau} [\tilde{u}(\tau') - \overline{u}]\, d\tau'\, d\tau. \tag{4.9}$$

5. Telegraph equation

Thacker (1976) showed that for a flow with two well-mixed layers and with negligible horizontal diffusivity, the bulk concentration $\bar{c}(x, t)$ satisfies a telegraph equation. Thus, his exact results provide a test of our model equation (1.6).

In this limit there is only one non-trivial eigenmode ψ_1. Thus the summations (3.4), (4.6) involve just a single term and equation (1.6), with $\bar{\kappa}$ neglected, becomes

$$\partial_t \bar{c} + \bar{u}\,\partial_x \bar{c} - \int_0^\infty u_1^2 \exp(-\lambda_1 \tau)\, \partial_x^2 \bar{c}(x - \tau u_{11}, t-\tau)\, d\tau = \bar{q}(x,t). \tag{5.1}$$

Applying the differential operator $(\partial_t + u_{11}\partial_x + \lambda_1)$ to both sides of this equation, we recover the telegraph equation

$$(\partial_t + u_{11}\partial_x + \lambda_1)(\partial_t \bar{c} + \bar{u}\,\partial_x \bar{c}) - \lambda_1^2 u_1^2 \partial_x^2 \bar{c} = (\partial_t + u_{11}\partial_x + \lambda_1)\bar{q}. \tag{5.2}$$

This is the equation (3) of Thacker (1976) with the minor generalizations that the bulk velocity $\bar{u}$ is non-zero, and the layer depths are unequal (i.e. $u_{11} \neq \bar{u}$).

A mathematically convenient feature of the telegraph equation is that it admits of exact solutions. Thus, we seek to approximate equation (1.6) in such a way that we obtain a telegraph equation, but with a minimum loss of accuracy. The close connection between the delay diffusion equation (1.6) and a telegraph equation can be seen from the exact expression

$$\begin{aligned}(\partial_t + v\partial_x + \lambda)(\partial_t + \bar{u}\partial_x - \bar{\kappa}\partial_x^2)\bar{c} - \partial_\tau D(0)\,\partial_x^2 \bar{c} \\ = (\partial_t + v\partial_x + \lambda)\bar{q} + \int_0^\infty [\partial_\tau^2 D + \lambda\,\partial_\tau D]\,\partial_x^2 \bar{c}\left(x - \int_0^\tau \tilde{u}, t-\tau\right) d\tau \\ + \int_0^\infty [v - \tilde{u}(\tau)]\,\partial_\tau D\,\partial_x^3 \bar{c}\left(x - \int_0^\tau \tilde{u}, t-\tau\right) d\tau.\end{aligned} \tag{5.3}$$

To eliminate the integral terms it suffices that $\partial_\tau D$ is proportional to $\exp(-\lambda\tau)$ and that $\tilde{u}(\tau')$ has the constant value v.

At large times the growth rate of the variance will be exact provided that $\partial_\tau D$ has the form

$$\partial_\tau D = \lambda D(\infty)\exp(-\lambda\tau). \tag{5.4}$$

Also, from equations (4.8), (4.9), we infer that the value of $\bar{c}^{(2)}$ and the growth rate for $\bar{c}^{(3)}$ will be asymptotically correct provided that the integrals

$$\int_0^\infty [D(\tau) - D(\infty)]\,d\tau, \quad \int_0^\infty \partial_\tau D \int_0^\tau [\tilde{u}(\tau') - \bar{u}]\,d\tau'\,d\tau, \tag{5.5}$$

have the correct values. The resulting selections for λ and v are given by weighted averages respectively of λ_m and u_{mn}:

$$\lambda \sum_{m=1}^{\infty} (u_m^2/\lambda_m^2) = \sum_{m=1}^{\infty} \lambda_m (u_m^2/\lambda_m^2), \tag{5.6}$$

$$v \sum_{m=1}^{\infty} (u_m^2/\lambda_m^2) = \sum_{m=1}^{\infty} u_{mm}(u_m^2/\lambda_m^2) + \sum_{m=1}^{\infty}\sum_{n\neq m} u_{mn}(u_m u_n/\lambda_m \lambda_n). \tag{5.7}$$

Chatwin (1970) showed that at large times the variance and skewness can be expressed in terms of a single function $g(y,z)$:

with
$$\left.\begin{aligned} \nabla.(\kappa\nabla g) &= \bar{u} - u, \\ \bar{g} = 0, \quad \text{and} \quad \kappa \mathbf{n}.\nabla g &= 0 \quad \text{on} \quad \partial A. \end{aligned}\right\} \tag{5.8}$$

Physically g can be interpreted as being the shape factor for the concentration variations across the flow in the well-mixed stage. Guided by Chatwin's results, we find that the formulae (5.6), (5.7) for λ and v can be rewritten

$$\lambda = \overline{ug}/\overline{g^2}, \quad v = \overline{ug^2}/\overline{g^2}, \quad D(\infty) = \overline{ug}. \tag{5.9}$$

Thus, in keeping with the heuristic basis of the new method, v is the (constant) transport velocity associated with the longest persisting lateral concentration variations.

With the approximations (5.4), (5.9) and with $\overline{\kappa}$ neglected the longitudinal dispersion equation takes the form

$$(\partial_t + v\,\partial_x + \lambda)(\partial_t + \overline{u}\,\partial_x)\,\bar{c} - \lambda D(\infty)\,\partial_x^2 \bar{c} = (\partial_t + v\,\partial_x + \lambda)\,\bar{q}. \tag{5.10}$$

This equation is hyperbolic with characteristic velocities

$$u_\pm = \tfrac{1}{2}(v+\overline{u}) \pm \{\lambda D(\infty) + \tfrac{1}{4}(v-\overline{u})^2\}^{\frac{1}{2}}. \tag{5.11}$$

The equivalent two-layer flow is

$$\left.\begin{aligned} &\text{area fraction } \tfrac{1}{2}(1 - s/[1+s^2]^{\frac{1}{2}}) \text{ with velocity } u_+, \\ &\text{area fraction } \tfrac{1}{2}(1 + s/[1+s^2]^{\frac{1}{2}}) \text{ with velocity } u_-, \end{aligned}\right\} \tag{5.12}$$

where s is the skewness parameter

$$s = \tfrac{1}{2}(v-\overline{u})/[\lambda D(\infty)]^{\frac{1}{2}} = \tfrac{1}{2}\overline{(u-\overline{u})\,g^2}/\overline{ug}(\overline{g^2})^{\frac{1}{2}}. \tag{5.13}$$

Thus, the characteristic velocities are precisely the flow velocities in the two layers. Also, the tendency to develop positive or negative skewness can be related to whether the smaller fraction of the flow is fast or slow moving (i.e. the tails of the contaminant distribution are associated with the smaller layer of fluid).

In axes moving with the bulk velocity $\overline{u}$, the fundamental solution of the telegraph equation (5.10) can be written

$$\bar{c} = \frac{(\partial_t + (v-\overline{u})\,\partial_x + \lambda)}{2[\lambda D(\infty) + \tfrac{1}{4}(v-\overline{u})^2]^{\frac{1}{2}}} \left\{ I_0(R)\,[H(x-(u_- - \overline{u})\,t) - H(x-(u_+ - \overline{u})\,t)] \right.$$
$$\left. \times \exp\left(- \frac{[\tfrac{1}{2}D(\infty)\,\lambda^2 t + \tfrac{1}{4}(v-\overline{u})\,\lambda x]}{[\lambda D(\infty) + \tfrac{1}{4}(v-\overline{u})^2]} \right) \right\}, \tag{5.14}$$

with

$$R^2 = \frac{\lambda^3 D(\infty)\,[\lambda D(\infty)\,t^2 + (v-\overline{u})\,xt - x^2]}{4[\lambda D(\infty) + \tfrac{1}{4}(v-\overline{u})^2]^2}. \tag{5.15}$$

Here I_0 is the modified Bessel function of order zero, and H is the unit step function which serves to indicate that the contaminant is confined between the extreme characteristics. Figures (1 *a*, *b*, *c*) show the development of the solution when the skewness parameter has the values $s = 0, \frac{1}{2}, 1$. For negative s the profiles are mirror images about the centroid position $x = 0$. The concentration spikes at the extreme characteristics can be interpreted as an exaggerated counterpart of the tendency for an exponentially decreasing quantity of contaminant to be carried at the maximum and minimum flow velocities (Sullivan 1971; Chatwin 1971, 1973). It is noteworthy that even at large values of λt the profiles have not yet attained the eventual Gaussian shape.

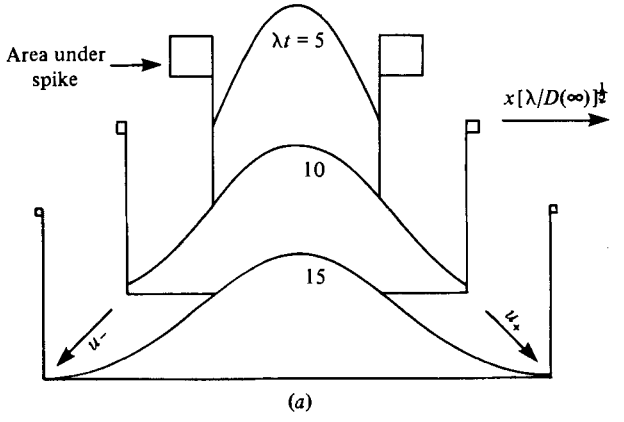

(*a*)

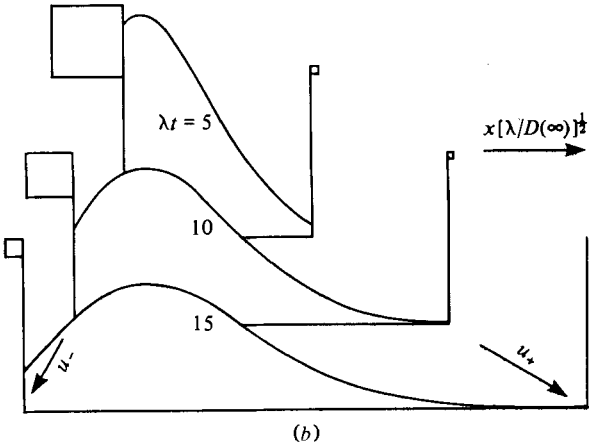

(*b*)

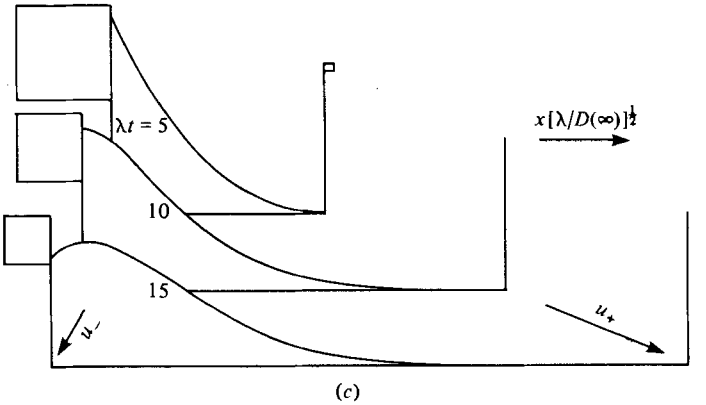

(*c*)

FIGURES 1 (*a–c*). Telegraph equation solutions for the dispersion of a sudden discharge when the skewness parameter has the values 0, ½, 1.

6. Method of application

To derive the delay-diffusion equation (1.6) for a given flow situation, the order of procedure is as follows:

(i) Determine the velocity field and the eigenfunctions ψ_m;

(ii) Use the formulae (3.6) and (3.4) to calculate the delay-dispersion function $\partial_\tau D$;

(iii) Evaluate the coefficients u_{mn}, and solve equation (4.6) for the velocity shift $\tilde{u}(\tau')$.

Alternatively, if asymptotic rather than exact moments are acceptable, then we can use the simpler procedure:

(i) Determine the velocity field $u(y,z)$ and the shape factor $g(y,z)$;

(ii) Use the formulae (5.9) to calculate the decay rate λ and the constant velocity shift v.

The remainder of this paper gives three illustrative examples of these procedures.

7. Poiseuille pipe flow

For laminar flow in a circular pipe of radius a we have

$$u = 2\bar{u}[1-(r/a)^2] \quad \text{with} \quad G = 8\bar{u}\nu/a^2. \tag{7.1}$$

The circular symmetry means that we can restrict our attention to pure radial eigenmodes:

$$\left.\begin{aligned} \psi_m/(\overline{\psi_m^2})^{\frac{1}{2}} &= J_0(\gamma_m(r/a))/J_0(\gamma_m), \\ J_0'(\gamma_m) &= 0, \quad \lambda_m = \gamma_m^2\kappa/a^2, \end{aligned}\right\} \tag{7.2}$$

with

where J_0 is the zero-order Bessel function of the first kind.

The drag forces are uniform around the pipe, thus from equation (3.6) we find

$$u_m = -8\bar{u}/\gamma_m^2. \tag{7.3}$$

Substituting this result into equation (3.4) we arrive at the formula

$$\partial_\tau D = 64\bar{u}^2 \sum_{m=1}^{\infty} \gamma_m^{-4} \exp(-\gamma_m^2\kappa\tau/a^2), \tag{7.4}$$

(see figure 2) in agreement with the work of Aris (1956, § 4). In particular, we record that

$$\partial_\tau D(0) = \overline{(u-\bar{u})^2} = \tfrac{1}{3}\bar{u}^2. \tag{7.5}$$

From Gill & Sankarasubramanian (1972, equation (33)), or by direct calculation, we can deduce that

$$u_{mm} = \tfrac{4}{3}\bar{u}, \quad u_{mn} = -8\bar{u}(\gamma_m^2+\gamma_n^2)/(\gamma_m^2-\gamma_n^2)^2 \quad \text{for} \quad m \neq n. \tag{7.6}$$

Using these values in equation (4.6) we find that $\tilde{u}(\tau')$ has the time-dependence shown in figure 3. A distinctive feature is that $\tilde{u}-\bar{u}$ is initially zero. Thus, for a symmetric discharge the concentration distribution initially remains symmetric. However, as τ' becomes larger the velocity shift $\tilde{u}(\tau')-\bar{u}$ becomes positive and the skewness develops towards the front. Qualitatively this is what we could anticipate from the fact that the smaller fraction of the flow (near the axis) is fast-moving.

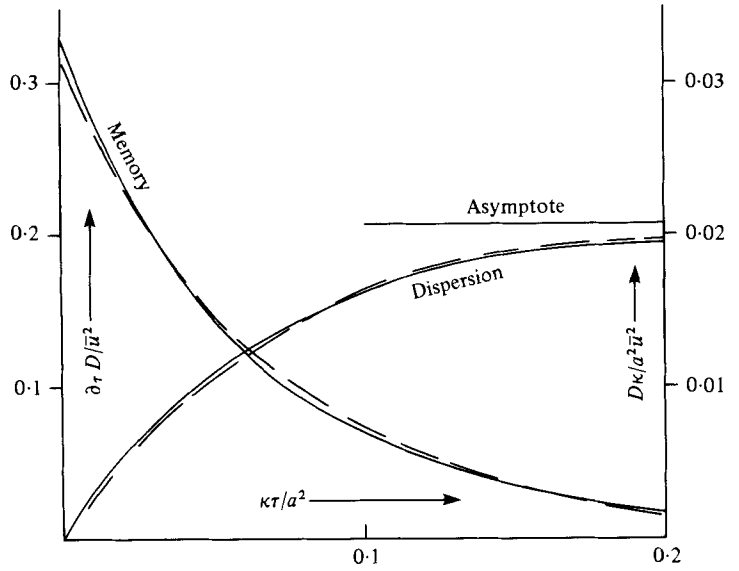

FIGURE 2. Exact (——) and telegraph equation approximations (— —) to the memory function $\partial_\tau D$ and the shear dispersion coefficient D for Poiseuille pipe flow.

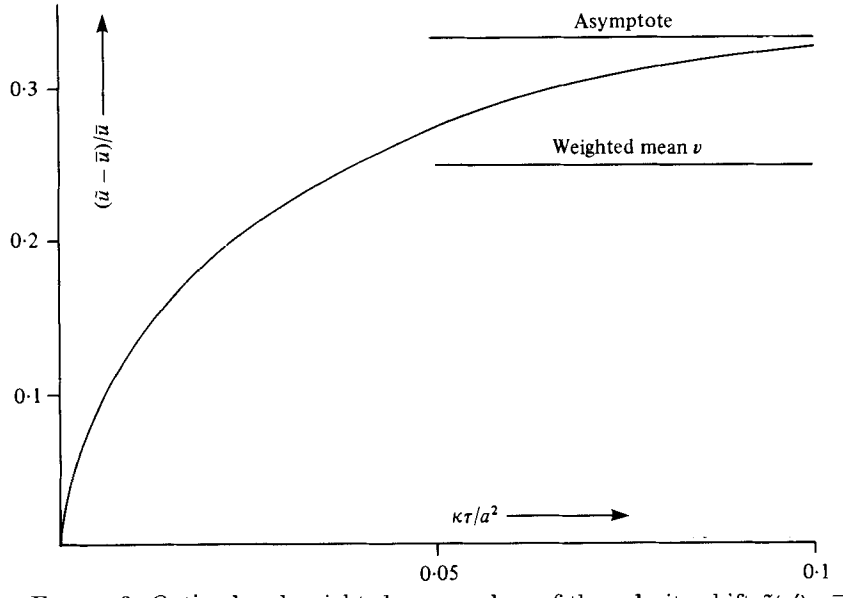

FIGURE 3. Optimal and weighted-mean values of the velocity shift $\tilde{u}(\tau')-\bar{u}$ for Poiseuille pipe flow.

To apply the telegraph-equation analysis, we first need to calculate the shape factor g:

$$g = \frac{\bar{u}a^2}{24\kappa}\{2-6(r/a)^2+3(r/a)^4\} \tag{7.7}$$

(Chatwin 1970, equation (4.1)). Performing the cross-sectional averages (5.9), we then arrive at the results

$$\lambda = 15\kappa/a^2, \quad v = \tfrac{5}{4}\bar{u}, \quad D(\infty) = \bar{u}^2a^2/48\kappa. \tag{7.8}$$

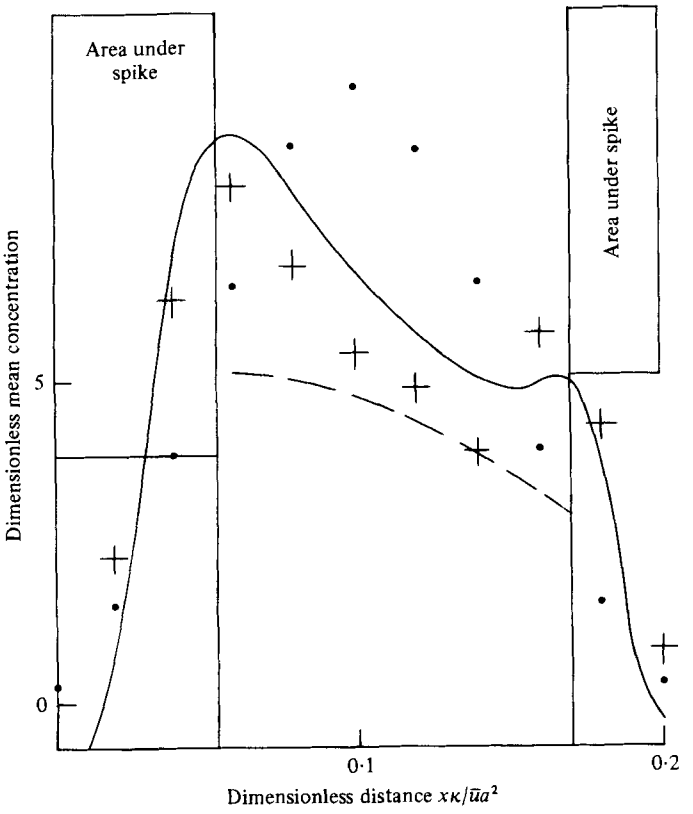

FIGURE 4. Exact (——), delay-diffusion (+ + +), Gaussian (· · ·) and telegraph equation (— —) concentration profiles at a time $0{\cdot}1\ a^2/\kappa$ after discharge in Poiseuille pipe flow.

Thus, the telegraph equation (5.4) takes the form

$$(\partial_t + \tfrac{5}{4}\bar{u}\,\partial_x + 15\kappa/a^2)(\partial_t \bar{c} + \bar{u}\,\partial_x \bar{c}) - (5\bar{u}^2/16)\,\partial_x^2 \bar{c} = (\partial_t + \tfrac{5}{4}\bar{u}\,\partial_x + 15\kappa/a^2)\,\bar{q}. \quad (7.9)$$

By construction the telegraph equation yields a very accurate description of the contaminant distribution at large times, with exact results for the area, centroid variance and skewness. Thus, it is of considerable interest to ascertain at what stage the model equation (7.9) becomes useful. Figure 4 compares the solution at $\lambda t = 1{\cdot}5$ with the numerical results of Gill & Ananthakrishnan (1967) and with the Gaussian solution of equation (1.1). The concentration spikes are unrealistic although their positions do correspond closely to the double-peaked structure of the numerical solution. The Gaussian solution exhibits none of this asymmetry. Indeed, it has to be admitted that at this comparatively early stage of the dispersion process neither the diffusion equation (1.1) nor the telegraph equation (7.9) can be regarded as giving adequate predictions. Of course, the delay-diffusion equation (1.6) is far superior to either of these simple models, but with the disadvantage of numerical rather than analytic solutions.

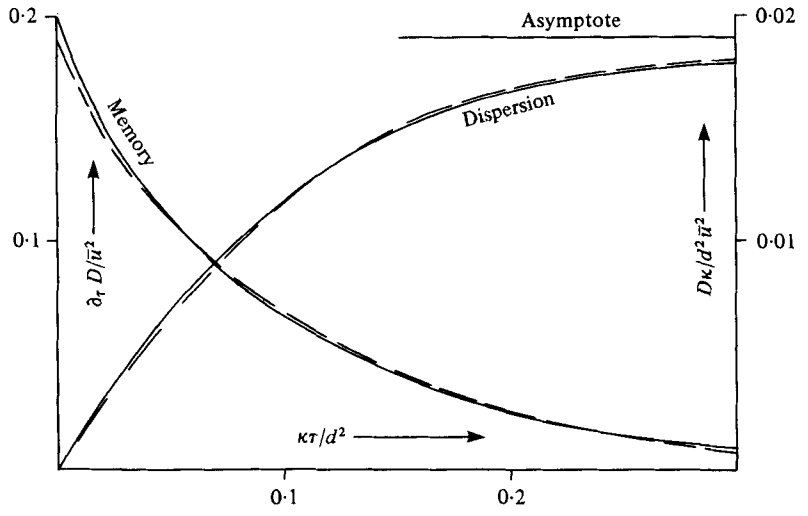

FIGURE 5. Exact (——), and telegraph equation approximations (— —) to the memory function $\partial_\tau D$ and the shear dispersion coefficient D for plane Poiseuille flow.

8. Plane Poiseuille flow

For laminar flow between parallel plates we have

$$u = \tfrac{3}{2}\bar{u}[1-(y/d)^2] \quad \text{with} \quad G = 3\bar{u}\nu/d^2, \tag{8.1}$$

where $2d$ is the plate separation. The symmetry of the velocity profile about $y = 0$ means that it suffices to involve only the even eigenmodes

$$\psi_m/(\overline{\psi_m^2})^{\frac{1}{2}} = \sqrt{2}\cos(m\pi y/d), \quad \lambda_m = m^2\pi^2\kappa/d^2. \tag{8.2}$$

Using these results in equation (3.6) we deduce that

$$u_m = (-1)^{m+1}\,3\sqrt{2}\,\bar{u}/m^2\pi^2, \tag{8.3}$$

and the delay dispersion function (3.4) is given by

$$\partial_\tau D = \frac{18}{\pi^4}\bar{u}^2 \sum_{m=1}^{\infty} m^{-4}\exp(-m^2\pi^2\kappa\tau/d^2) \tag{8.4}$$

(see figure 5). When we allow for the different definition of the plate separation, this agrees with the result derived by Dewey & Sullivan (1979, equation (32)).

To evaluate the coefficients u_{mn}, we first note that

$$\psi_m\psi_n/(\overline{\psi_m^2})^{\frac{1}{2}}(\overline{\psi_n^2})^{\frac{1}{2}} = \cos((m-n)\pi y/d) + \cos((m+n)\pi y/d). \tag{8.5}$$

It then follows from the definitions (3.2), (4.1) that

$$\left.\begin{aligned} &u_{mm} = \bar{u} + u_{2m}/\sqrt{2}, \quad u_{mn} = (u_{m-n} + u_{m+n})/\sqrt{2}, \\ \text{i.e.} \quad &u_{mm} = \bar{u}\left(1 - \frac{3}{4m^2\pi^2}\right), \quad u_{mn} = \frac{6(m^2+n^2)}{(m^2-n^2)^2}\frac{(-1)^{m+n+1}}{\pi^2}\bar{u}. \end{aligned}\right\} \tag{8.6}$$

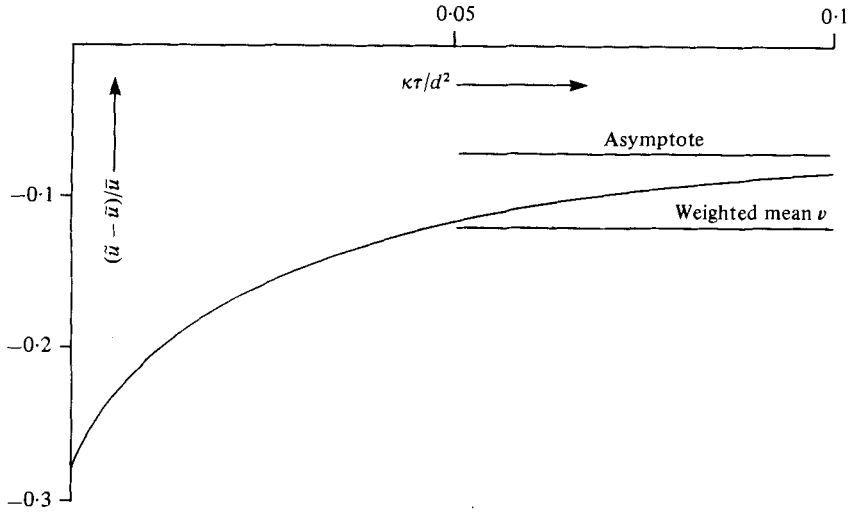

FIGURE 6. Optimal and weighted-mean values of the velocity shift $\tilde{u}(\tau')-\bar{u}$ for plane Poiseuille flow.

Figure 6 shows the time-dependence of $\tilde{u}(\tau')$ which results from substituting these coefficients into equation (4.6). In the limits of small and of large times we have

$$\tilde{u}(0)-\bar{u} = -\tfrac{2}{7}\bar{u}, \quad u(\infty)-\bar{u} = -3\bar{u}/4\pi^2. \tag{8.7}$$

Thus, there is initially a strong tendency to develop negative skewness which diminishes at later times. The sign of the skewness is precisely what we would expect from the fact that it is the smaller fraction of the flow (near the walls) that is slow-moving.

The shape factor $g(y)$ required for the derivation of the telegraph-equation approximation is given by

$$g = \frac{\bar{u}d^2}{120\kappa}\{7-30(y/d)^2+15(y/d)^4\}, \tag{8.8}$$

and from equation (5.9) we arrive at the results

$$\lambda = 10\kappa/d^2, \quad v = 29\bar{u}/33, \quad D(\infty) = \bar{u}^2d^2/105\kappa. \tag{8.9}$$

Hence, the telegraph equation for longitudinal dispersion in plane Poiseuille flow is

$$(\partial_t+\tfrac{29}{33}\bar{u}\,\partial_x+10\kappa/d^2)(\partial_t\bar{c}+\bar{u}\,\partial_x\bar{c})-(4\bar{u}^2/21)\,\partial_x^2\bar{c} = (\partial_t+\tfrac{29}{33}\bar{u}\,\partial_x+10\kappa/d^2)\,\bar{q}. \tag{8.10}$$

Figure 7 compares the solution at $\lambda t = 4$ with the numerical results of Jayaraj & Subramanian (1978), and with the Gaussian solution of equation (1.1). As was the case with figure 4, the two-layer character of the telegraph equation has the unrealistic consequence of concentration spikes moving with the layer velocities. However, at this later stage in the dispersion process, the area under the spikes has become relatively small and the telegraph-equation solution is much more accurate than the Gaussian profile. Again, the very best accuracy is achieved by the numerical solution of the delay-diffusion equation.

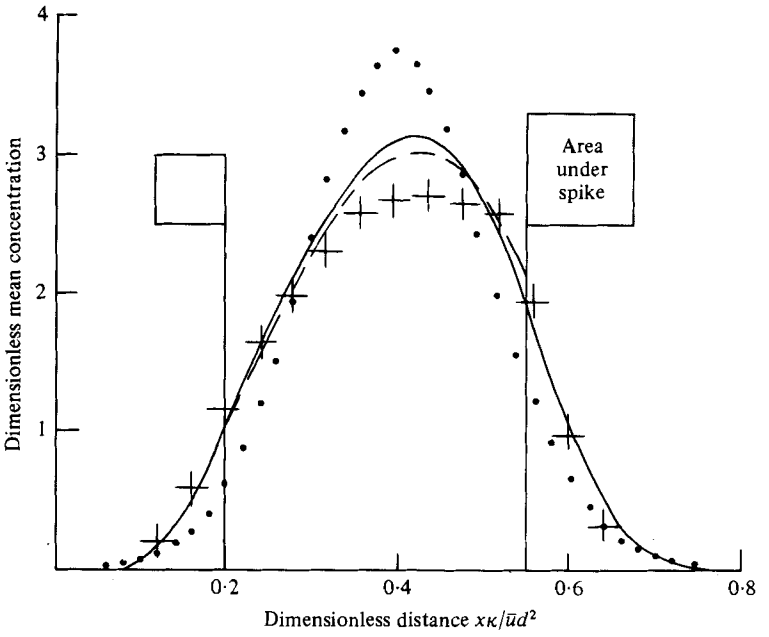

FIGURE 7. Exact (——), delay-diffusion (+ + +), Gaussian (· · ·), and telegraph equation (— —) concentration profiles at a time $0{\cdot}4\, d^2/\kappa$ after discharge in plane Poiseuille flow.

9. Turbulent open-channel flow

As our final example we take the flow to have the classical logarithmic velocity profile

$$u = \bar{u} + (u_*/k)\,(1 + \ln(1 + z/h)) \quad \text{with} \quad G = u_*^2/h, \tag{9.1}$$

where u_* is the friction velocity, h the water depth, and k is von Kármán's constant (about 0.4). The corresponding model for the eddy diffusivities is

$$\kappa = \nu = k u_* h (1 + z/h)\,(-z/h). \tag{9.2}$$

The eigenfunctions for the decay of vertical concentration variations turn out to be the Legendre polynomials

$$\psi_m / \overline{(\psi_m^2)^{\frac{1}{2}}} = (2m+1)^{\frac{1}{2}} P_m(2(z/h) + 1), \tag{9.3}$$

with

$$\lambda_m = m(m+1)\, k u_*/h.$$

The drag is only at the channel bed $z = -h$, so from equation (3.6) we deduce that

$$u_m = (2m+1)^{\frac{1}{2}}\,(-1)^{m+1} u_*/km(m+1). \tag{9.4}$$

Substituting this expression into equation (3.4), we get

$$\partial_\tau D = \frac{u_*^2}{k^2} \sum_{m=1}^{\infty} \frac{(2m+1)}{m^2(m+1)^2} \exp(-m(m+1)\, k u_* \tau/h), \tag{9.5}$$

(see figure 8). In particular, we note that

$$\partial_\tau D(0) = u_*^2/k^2.$$

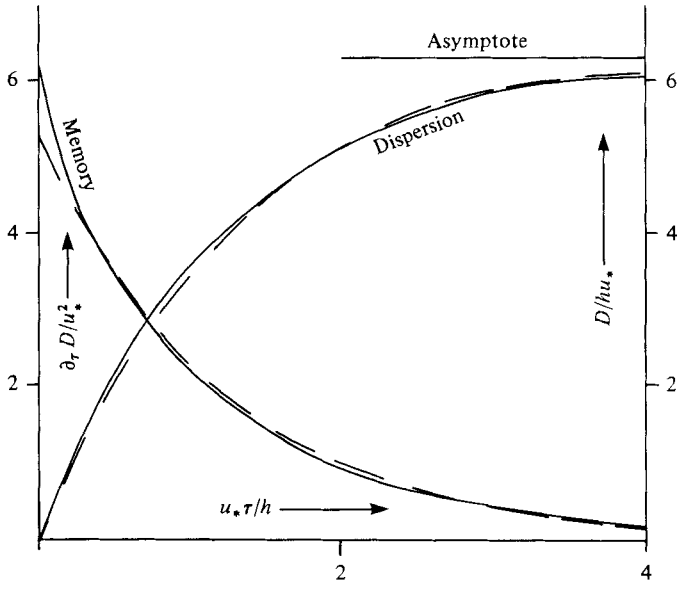

FIGURE 8. Exact (——) and telegraph equation approximations (— —) to the memory function $\partial_\tau D$ and the shear dispersion coefficient D for turbulent open-channel flows.

To evaluate the coefficients u_{mn}, we first introduce the Wronskian

$$W = P_m dP_n/dz - P_n dP_m/dz. \tag{9.6}$$

This satisfies the first-order differential equation

$$(d/dz)\,((h+z)(-z)W) = -(n-m)(n+m+1)P_n P_m. \tag{9.7}$$

If we multiply through by the velocity profile (9.1) and integrate the left-hand side by parts, then we arrive at

$$u_{mn} = \frac{u_*}{k}\frac{(2m+1)^{\frac{1}{2}}(2n+1)^{\frac{1}{2}}(-1)^{m-n+1}}{|n-m|\,(m+n+1)} \quad \text{for} \quad m \neq n. \tag{9.8}$$

A more lengthy argument, based upon simple induction, yields the complementary result

$$u_{mm} = \bar{u} - \frac{u_*}{k}\left[-\frac{2m}{2m+1} + 2\sum_{j=1}^{2m}\frac{(-1)^{j-1}}{j}\right]. \tag{9.9}$$

Figure 9 shows the time dependence of $\tilde{u}(\tau')$ obtained by substituting these results (9.8), (9.9) into equation (4.6). In the limits of small and or large times we have

$$\tilde{u}(0) - \bar{u} = -2(u_*/k), \quad \tilde{u}(\infty) - \bar{u} = -\tfrac{1}{3}u_*/k. \tag{9.10}$$

Thus, at all stages the tendency is to develop negative skewness but with the effect most pronounced early on. Again, this agrees with our general rule that it is the smaller fraction of the flow (in this case the wall layer) which determines the tail of the contaminant distribution.

The shape factor $g(z)$ for the longest persisting concentration variations across the flow is given by

$$g = \frac{h}{k^2}\left\{1 - \int_{-h}^{z}\frac{\ln(1+z/h)}{z}\,dz\right\}. \tag{9.11}$$

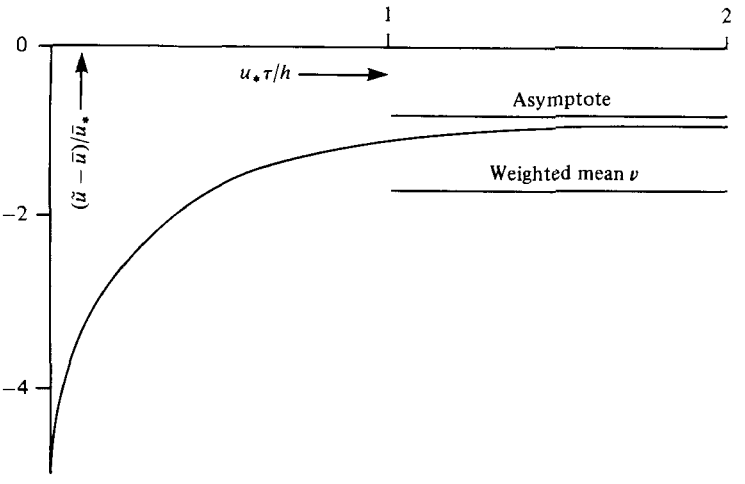

FIGURE 9. Optimal and weighted-mean values of the velocity shift $\tilde{u}(\tau')-\bar{u}$ for turbulent open-channel flows.

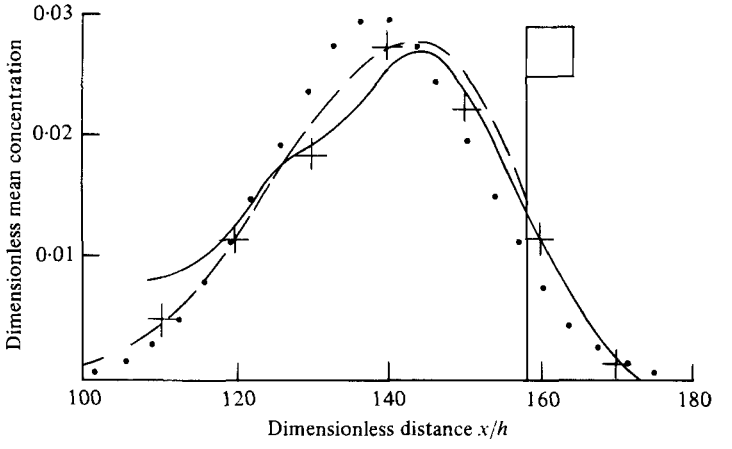

FIGURE 10. Experimental (——), delay-diffusion (+ + +), Gaussian (· · ·) and telegraph equation (— —) concentration profiles at a time 9·9 h/u_* after discharge in turbulent open-channel flow.

Chatwin (1970) gives results correct to two significant figures for the integrals $\overline{g^2}$, $\overline{ug^2}$. Improving the accuracy to four figures we arrive at the results

$$\lambda = 2{\cdot}107ku_*/h, \quad v = \bar{u} - 0{\cdot}6781u_*/k, \quad D(\infty) = 0{\cdot}4041hu_*/k^3. \tag{9.12}$$

If we take $k = 0{\cdot}4$, then the telegraph equation for longitudinal dispersion in turbulent open-channel flow takes the form

$$[\partial_t + (\bar{u} - 1{\cdot}7u_*)\,\partial_x + 0{\cdot}84u_*/h][\partial_t\bar{c} + \bar{u}\,\partial_x\bar{c}] - 5{\cdot}3u_*^2\,\partial_x^2\bar{c} = [\partial_t + (\bar{u} - 1{\cdot}7u_*)\,\partial_x + 0{\cdot}84u_*/h]\bar{q}. \tag{9.13}$$

Elder (1959, figure 4) presents experimental results for $\bar{c}(x,t)$ when the parameter values are given by

$$\bar{u} = 14u_*, \quad t = 9{\cdot}9h/u_*, \quad k = 0{\cdot}41. \tag{9.14}$$

Figure 10 compares these results with the telegraph-equation solution and with the

Gaussian solution of equation (1.1). As has been further explored by Sullivan (1971), the slow-moving fluid near the wall drags out the contaminant distribution into a distinctly non-Gaussian profile. However, there is a reasonable overall agreement with the telegraph-equation solution. Indeed, there is only minor improvement if we use the numerical solution of the delay-diffusion equation.

This work owes much to a stimulating discussion with Malcolm Davidson (Australian Atomic Energy Commission). Also, I wish to thank B.P. for financial support through the award of the Royal Society British Petroleum Company Limited Senior Research Fellowship.

REFERENCES

ARIS, R. 1956 On the dispersion of a solute in a fluid flowing through a tube. *Proc. Roy. Soc.* A **235**, 67–77.

CHATWIN, P. C. 1970 The approach to normality of the concentration distribution of a solute in solvent flowing along a pipe. *J. Fluid Mech.* **43**, 321–352.

CHATWIN, P. C. 1971 On the interpretation of some longitudinal dispersion experiments. *J. Fluid Mech.* **48**, 689–702.

CHATWIN, P. C. 1973 A calculation illustrating effects of the viscous sub-layer on longitudinal dispersion. *Quart. J. Mech. Appl. Math.* **26**, 427–439.

DE GANCE, A. E. & JOHNS, L. E. 1978 The theory of dispersion of chemically active solutes in a rectilinear flow field. *App. Sci. Res.* **34**, 189–225.

DEWEY, R. & SULLIVAN, P. J. 1979 Longitudinal dispersion in flows that are homogeneous in the streamwise direction. *Z. angew. Math. Phys.* **30**, 601–613.

ELDER, J. W. 1959 The dispersion of marked fluid in turbulent shear flow. *J. Fluid Mech.* **5**, 544–560.

GILL, W. M. & ANANTHAKRISHNAN, V. 1967 Laminar dispersion in capillaries: Part 4. The slug stimulus. *A.I.Ch.E. J.* **13**, 801–807.

GILL, W. M. & SANKARASUBRAMANIAN, R. 1970 Exact analysis of unsteady convective diffusion. *Proc. Roy. Soc.* A **316**, 341–350.

GILL, W. M. & SANKARASUBRAMANIAN, R. 1972 Dispersion of non-uniformly distributed time-variable continuous sources in time-dependent flow. *Proc. Roy. Soc.* A **327**, 191–208.

JAYARAJ, K. & SUBRAMANIAN, R. S. 1978 On relaxation phenomena in field-flow fractionation. *Sep. Sci. Tech.* **13**, 791–817.

SULLIVAN, P. J. 1971 Longitudinal dispersion within a two-dimensional turbulent shear flow. *J. Fluid Mech.* **49**, 551–576.

TAYLOR, G. I. 1953 Dispersion of soluble matter in solvent flowing slowly through a tube. *Proc. Roy. Soc.* A **219**, 186–203.

TAYLOR, G. I. 1954 The dispersion of matter in turbulent flow through a pipe. *Proc. Roy. Soc.* A **223**, 446–468.

TAYLOR, G. I. 1959 The present position in the theory of turbulent diffusion. *Adv. Geophys.* **6**, 101–111.

THACKER, W. C. 1976 A solvable model of shear dispersion. *J. Phys. Oceanog.* **6**, 66–75.